05,16

Kerr effect transformation caused by proximity effect in bilayer structures of magnetic and nonmagnetic transition metals

© V.A. Skidanov

National Research Center „Kurchatov Institute“,
Moscow, Russia

E-mail: skidanov@ippm.ru

Received October 29, 2025
Revised January 20, 2026
Accepted January 21, 2026

Hysteresis loops in a low-frequency alternating magnetic field in films of nonmagnetic transition metals deposited on the surface of a ferromagnetic metal have been experimentally observed using the magneto-optical transverse Kerr effect. The shape of the hysteresis is identical to the shape of the loops from the ferromagnetic layer and is observed in films of normal metals, even when their thickness h significantly exceeds the depth of light penetration. The dependence of the Kerr signal on the thickness h of a non-magnetic metal is alternating and varies depending on the composition of the ferromagnetic. Experimental data allow estimating the length of spin diffusion in tantalum for unexcited electrons — $\lambda_{sf} = 50 \pm 10$ nm, which is 2−4 times the depth of light penetration into transition metals. The observed effect decreases with electron filling of the outer d-shell of a normal metal ($d^2 \rightarrow d^9$) and disappears in metals with an empty or completely filled d-shell. Films of Al ($3d^0$), Cu ($3d^{10}$) and Au ($5d^{10}$) on the surface of a ferromagnetic metal have only a shielding effect. The Kerr signal from a ferromagnetic metal film also changes in the presence of a normal metal sublayer and can be amplified several times.

Keywords: phenomena caused by proximity effect, transverse Kerr effect, spin diffusion, hysteresis loop.

DOI: 10.61011/PSS.2026.01.63244.305-25

1. Introduction

Phenomena at the interface between magnetic and nonmagnetic media have attracted increasing attention in the last decade [1]. The possibility of transferring the spin ordering from the ferromagnetic metal F to the ordinary metal N is of particular interest from the point of view of important applications. The magnetization induced by contact with a ferromagnetic metal has been studied in metals such as Pt, Pd, Ir, Ru, W, and Ta due to their proximity to a ferromagnetic junction or large spin-orbit coupling [2–5]. The magnetic moment in Pd induced by proximity to Fe was found in the Fe|Pd structure at a depth of up to 2 nm in Pt (in the Fe|Pt structure and a much smaller effect in Ni|Pt). The abnormal Nernst effect has been identified in the Pt|NiFe structure. An ultrahigh mobility of domain boundaries in thin Co and CoNi films with perpendicular anisotropy deposited on a Pt sublayer has also been found, which is explained by the formation of a helicoidal magnetic moment at the interface.

Experimental studies were carried out using the methods of X-ray resonant magnetic scattering, X-ray magnetic circular dichroism and absorption spectroscopy, polarized neutron reflectometry, and ferromagnetic resonance [6–11]. Spin resonance was used to study spin mixing near the interface $F-N$ in both ferromagnetic (Co, CoFeB) and heavy metal (Pt, W) layers in order to quantify the parameters of spin transfer into a nonmagnetic metal. The results are very contradictory. For example, in platinum, the polarization of free electrons at the level of $5 \cdot 10^{-12}\,\mu_B$ per atom was detected only under conditions of injection through the interface of electrons with a current density of 1 A/cm^2 [7]. The transition to the ferromagnetic state (platinum and tungsten) is not discussed. The authors of Ref. [8] determined the magnitude of magnetization in platinum of the order of $1\,\mu_B$ at a depth of 1 nm in the structure of Fe|Pt.

In any case, the magnetization of a normal metal is localized within a few atomic layers from the interface. Therefore, the mechanism of mixing remains unclear, in particular, due to the lack of information about the type of mixing in such structures — atomic, electronic, or purely exchange interaction of ferromagnetic and nonmagnetic metal ions.

Long-range effects were investigated at the ferromagnetic-superconductor interface. Two types of proximity effects have been found: the penetration of a magnetic field into a superconductor, associated with the electromagnetic mechanism [12,13], and the penetration of superconductivity into the ferromagnetic layer due to the triplet pairing of electrons [14,15]. Recently, deep diffusion of the orbital angular momentum of electrons $\lambda_{or} \approx 80$ nm into tungsten in the two-layer structure Ni|W was discovered [16].

Optical phenomena in $F|N$-bilayers were used to increase the sensitivity of biochips [17] by modulating a plasmon wave in a noble metal (in Fe|Ag structures) by an external magnetic field [18] or, conversely, to amplify the Kerr signal due to the interaction of a light wave in the F-layer with a plasmon wave, propagating in the noble metal (in Au|Co|Au structures) [19–22].

It should be noted that spin diffusion from iron to a 6 nm thick tin layer in the Fe|Sn|Fe film structure was previously experimentally observed using the Mössbauer effect in Sn^{119} [23]. E.K. Zavoysky predicted then that the long-range diffusion of polarized electrons from a ferromagnetic metal across the interface could provide an opportunity to observe an EPR signal from diamagnetic metals [24]. At the same time, A.G. Aronov estimated the diffusion depth of polarized electrons in aluminum at $\lambda_{sf} \approx 10^4$ nm [25].

In this work, the optical transverse Kerr effect is used to study the diffusion of polarized electrons across the interface in the $N|F$-bilayer of transition normal N and ferromagnetic F metals. A new unexpected phenomenon of long-range magneto-optical activity found in transition nonmagnetic metals in contact with ferromagnetic metals is presented.

2. Experimental procedure

The objects of the study were made by magnetron sputtering of metal targets. Parallel strips of ferromagnetic metals (permalloy Ni80-Fe20 and pure iron) of various thicknesses t in the range of 5–40 nm were sputtered onto glass substrates using masking coatings. The ferromagnetic layers were sputtered in an external magnetic field to create anisotropy with the axis of light magnetization in the plane of the layer. Then, strips of non-magnetic transition metal of various thicknesses h in the range of 5–180 nm were sputtered perpendicularly to form a regular matrix of two-layer rectangles (5×5 mm) with a set of pairs of thickness values (t, h), as shown in Figure 1.

The amplitudes of the complete hysteresis loops (Figure 2) $A(t, h)$ were recorded using the standard magneto-optical method (measurement of the transverse Kerr effect). An incandescent lamp with a stabilized power supply was used as a white light source. A silicon photodiode was used as a reflected light intensity sensor. The angle of incidence was 45°. The diameter of the light spot was ~ 3 mm. Although the thickness of the studied layers was significantly less than the wavelength of light, white light was used to avoid the effects of interference and/or resonant excitation of plasmon waves. All measurements were carried out at the same level of reflected light intensity, which was strictly controlled by the photodiode to avoid uncertainty caused by differences in the thickness of objects and transparency values. Since the reflection coefficient increases with the thickness of the metal film, the intensity of the incident light was correspondingly reduced by controlling the lamp current for thicker structures. An external alternating magnetic field (50 Hz) was applied in the film plane and perpendicular to the optical plane using a pair of Helmholtz coils. The amplitude of the external field was sufficient to saturate the magnetization. All measured magneto-optical signals are normalized by the value of the signal from a Py film with a thickness of t exceeding the depth of light penetration into permalloy ($t \geq 40$ nm), unless otherwise specified. The measurements were carried out at room temperature.

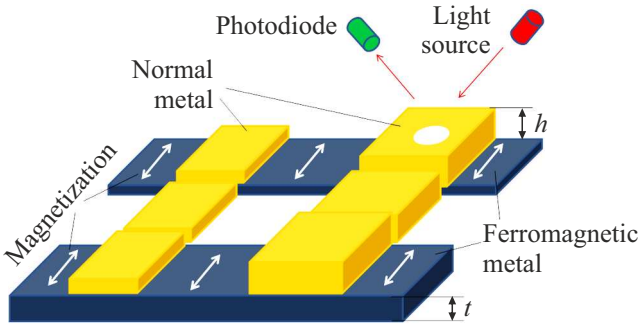

Figure 1. Kerr signal research scheme in $N|F$-bilayers.

3. Findings

For the first time, the phenomenon was observed when testing a Py film with a Cr protective layer on an installation for measuring coercive force using the transverse Kerr effect. The presence of a normal transition metal layer above the ferromagnetic metal significantly alters the magneto-optical response of the film. For a two-layer Cr|Py film, an inversion of the magneto-optical signal was observed compared with a single Py film (instead of an exponential decrease in the signal without changing its sign due to optical shielding of permalloy with a non-magnetic metal). In this case, the shape of the hysteresis loop of the Cr|Py structure repeated the shape of the hysteresis loop of the Py layer. The rotation of the external magnetic field from the axis of easy magnetization to the axis of difficult magnetization in the plane of the structure is accompanied by a synchronous transformation of the hysteresis loops of the single permalloy film and the Cr|Py structure, as shown in Figure 2. This indicates that the observed hysteresis loop in the Cr|Py structure is formed by a change in the magnetization in the permalloy layer.

Magneto-optical signal amplification with sign inversion was detected after applying a Ta layer on top of the Py film, as shown in the photographs (inset in Figure 3). To maintain a constant intensity of reflected light, the intensity of incident light when measuring the signal from the Ta|Py bilayer decreased controllably as the thicknesses of tantalum and permalloy increased.

The identity of the shape of the hysteresis loops suggests a conclusion about the purely optical nature of the signal conversion effect. However, the Kerr signal in the form of an observed hysteresis loop is also detected in the $h \geq 150$ nm thick Ta layer, at which light practically does not reach the ferromagnetic layer. The dependences of the signal amplitude on the thickness h of the nonmagnetic layer in two-layer Ta|Py structures demonstrate non-monotonic

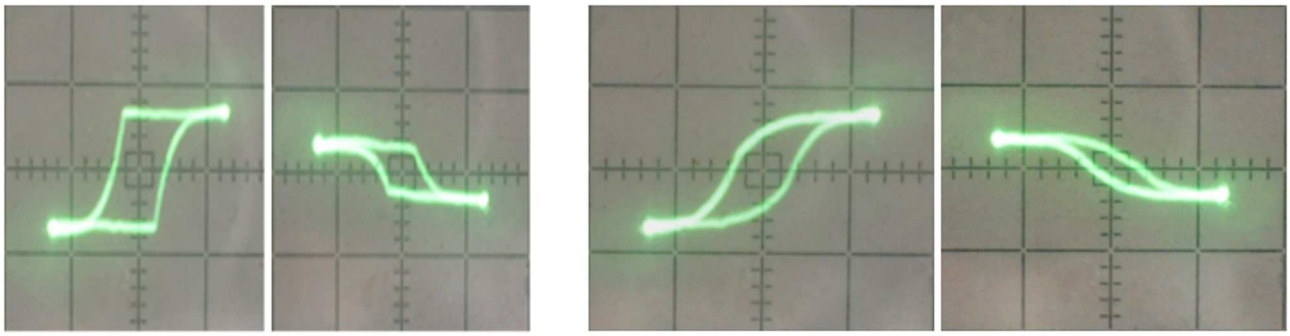

Figure 2. Kerr signals of changes in the magnetization of the Py film along *a, b*) easy and *c, d*) difficult axes for two neighboring objects: (*a*) and (*c*) — for single-layer film Py, $t = 15$ nm, (*b*) and (*d*) — for the Cr|Py structure, the thickness is Cr $h = 20$ nm. Calibration of the magnetic field amplitude along the x axis — 4 Oe/div.

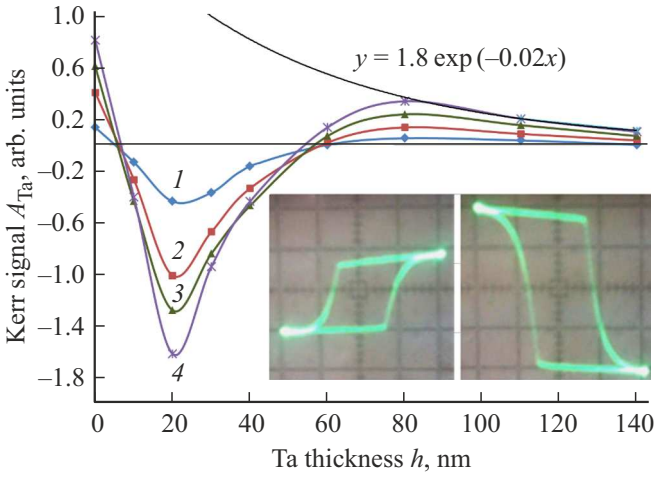

Figure 3. Dependences of the normalized signal amplitudes $A_{Ta}(h, t)$ from the film side Ta on the thickness h for thickness values Py t: curve *1* — 5 nm, *2* — 12 nm, *3* — 20 nm, *4* — 30 nm. Insert: on the left — magneto-optical signal from a single layer of Py, $t = 20$ nm, on the right — magneto-optical signal from a bilayer of Ta|Py, $h = t = 20$ nm. Calibration of the magnetic field amplitude along the x axis — 4 Oe/div.

behavior with sign changes instead of exponential decrease due to light absorption in the nonmagnetic layer, as shown for a number of values of Py thickness t in Figure 3.

A rapid decrease and inversion (sign change) of the Kerr signal are observed when the Ta thickness $h \approx 7$ nm is reached. The inverted signal reaches its maximum amplitude at $h \approx 20$ nm. A further increase in the thickness of the Ta layer is accompanied by a decrease in the amplitude of the inverted signal to zero at $h \approx 55$ nm, where the signal unexpectedly changes sign again, and then increases with the thickness of Ta to $h \approx 80$ nm, although the Ta film is completely opaque already at $h \geq 40$ nm. Exponential attenuation of the signal occurs only at $h > 80$ nm.

The effect of Ta on the magneto-optical signal was also observed in the Py|Ta configuration, when light falls on the Py layer, and the Ta layer is located under it, and is shown in Figure 4.

The Kerr signal decreases for all Py thickness values in the range of $t \leq 30$ nm, where the permalloy layer is partially transparent. The signals reach a minimum at $h \approx 20$ nm, which is consistent with the minimum values of the inverted signal in Figure 3. The total signal from the Py|Ta bilayer even changes sign for a thin transparent layer Py (thickness $t = 5$ nm) when the amplitude of the inverted signal generated in the Ta layer under permalloy exceeds the signal from the Py layer itself.

An increase in the thickness of Ta in the range of $h \geq 20$ nm leads to an increase in magneto-optical signals that exceed the signals from the isolated film Py (values at $h = 0$ in Figure 4). The signal magnitude increases even at $h \geq 40$ nm and reaches a maximum at $(t + h) \geq 70$ nm, i. e., Kerr signal sources are redistributed in the volume of the Py|Ta bilayer as the thickness of the lower tantalum layer changes, when the light intensity at the boundary with the substrate is negligible.

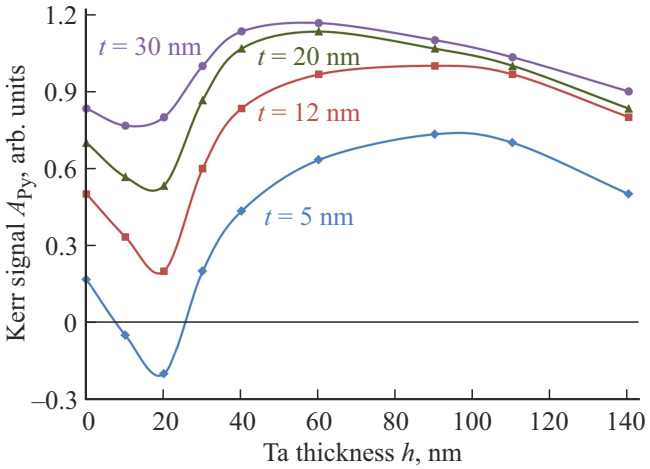

Figure 4. The dependences of the normalized signal amplitudes for the Py|Ta bilayer from the side of the Py layer $A_{Py}(h, t)$ on the thickness of the Tah layer for a set of thickness values t of Py.

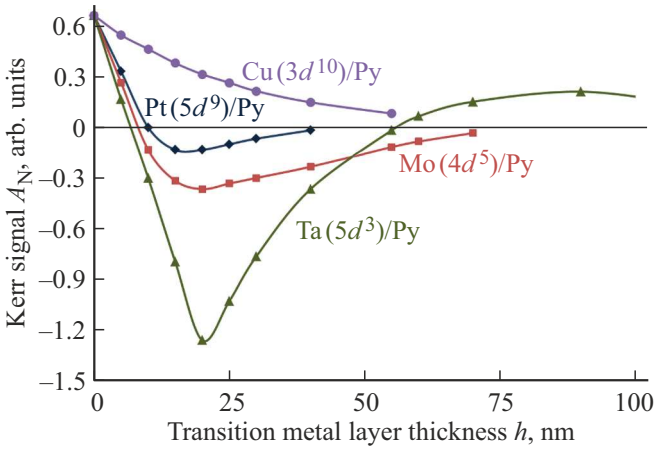

Figure 5. Dependences of normalized Kerr signals from normal transition metals $A_N(h)$ on their thickness values h, thickness Py $t = 20$ nm.

The largest — 5-multiple signal amplification is achieved for the thinnest film Py. This means that the Ta layer generates its own Kerr signal, which is closely related to the remagnetization of the Py layer. The gradual decrease in the signals in the range of $(t + h) \geq 100$ nm demonstrates the redistribution of the main electrons along the thickness of Ta with an increase of h and indicates a non-optical mechanism for changing the magneto-optical Kerr signal, since light does not penetrate the interface between the bilayer and the substrate.

The magnitude of the Kerr effect is determined by the presence of polarized electrons below the Fermi level and empty states for them in the d-band above the Fermi level E_F. The amplitude of the magneto-optical signal A is proportional to the difference in the number of transitions of basic and non-basic polarized electrons to empty states above the Fermi level, the probability of which is proportional to the product of the corresponding densities of states:

$$A \propto \iint [n_\uparrow(E)m_\uparrow(E+\hbar\omega) - n_\downarrow(E)m_\downarrow(E+\hbar\omega)]S(\omega)dEd\omega,$$

where $n_\uparrow(E)$ and $n_\downarrow(E)$ is the density of states of basic and non-basic polarized electrons, respectively, in the d-band below the Fermi level, $m\uparrow(E)$ and $m_\downarrow(E)$ are the densities of empty states for these electrons in the d-band above the Fermi level, $\hbar\omega$ is the energy of the absorbed photon, $S(\omega)$ is the spectrum of incident light. Integration of energy E is performed in the range from $(E_F - \hbar\omega_0)$ to $(E_F + \hbar\omega_0)$, and for ω — from 0 to the upper limit of the light spectrum $\hbar\omega_0$.

The Fermi level E_F in a transition metal is strictly determined by the degree of filling of the atomic d-shell. E_F monotonously shifts along the d-band of the scale of energy E as the d-shell of the element is filled, so that for Al (d^0) d-band is completely located above E_F $(n_{\uparrow\downarrow} = 0)$, and for Cu, Ag, Au (d^{10}) d-band is completely located below E_F $(m_{\downarrow\uparrow} = 0)$.

Experimental studies were carried out on a set of normal transition metals with different outer atomic shells 3d, 4d, and 5d (Ti, Cr, Mo, Ta, W, Re, Pt, Cu, and Au). It was found that the effect of a normal metal layer on the Kerr effect transformation strictly depends on the filling of the atomic d-shell. The effect of the Kerr signal conversion gradually decreases with the filling of the d-shell of a non-magnetic transition metal, as shown in Figure5.

The elements Cr $(3d^5)$, Mo $(4d^5)$ and Re $(5d^5)$ with different outer d-shells, but with the same filling, exhibit similar magneto-optical responses. The amplitude of the magneto-optical signal from the tungsten layer W $(5d^4)$ was found between Ta $(5d^3)$ and Mo $(4d^5)$ with the same thicknesses of non-magnetic metals. The smallest effect was observed for Pt $(5d^9)$ with the maximum inverted signal at $h \approx 15$ nm, which is consistent with the spin diffusion length $\lambda_{sf} = 11 \pm 3$ nm obtained in Ref. [7]. The largest amplitude of the inverted hysteresis loop signal was obtained from the Ti $(3d^2)$ layer above the Py layer.

Signal inversion was not observed for Cu and Au with completely filled d-shells and for Al with an empty 3d-shell. The dependence of the magneto-optical signal on the thickness of the Cu layer (Figure 5) demonstrates the effect of screening the Kerr signal occurring directly in the Py layer, with an exponential decrease of $A_{Cu}(h) \propto \exp(-\beta h)$, where $\beta^{-1} = 26.5 \pm 1.0$ nm is the depth of light penetration into copper.

At the same time, a twofold amplification of the magneto-optical signal from the Py film was detected in the presence of Cu or Au layers under it, in accordance with the result obtained in Ref. [26].

4. Discussion of the results

A natural hypothesis that can explain the behavior of the Kerr signal is the deep diffusion of polarized electrons at the Fermi level from Py into a normal metal, which has a number of empty states above the Fermi level in the d-band.

The band structure of permalloy is close to that of nickel Ni (d^8) with an almost filled d-band with little exchange splitting, and the Kerr signal from Py is relatively small. The concentration of nonbasic electrons in Py is prevalent at the Fermi level [27]. The basic and non-basic electrons located near the common Fermi level can easily diffuse through the interface Py$-N$. In this case, non-basic electrons also dominate in a normal metal in the immediate vicinity of the interface with Py, and provide a negative contribution to the total magneto-optical signals from the bilayers of N|Py and Py|N if the normal metal has empty states above the Fermi level.

According to the calculation results given in Ref. [28], the average velocity of the basic electrons in Ni and Fe is several times higher than the velocity of the non-basic electrons. The diffusive penetration of the main electrons into the volume of a normal metal occurs deeper, since with an equal lifetime of spin diffusion they diffuse to a

greater depth. Thus, the Kerr signals for the Ta|Py bilayers exhibit an inverse inversion and increase with growth h when $h > 40$ nm (Figure 3). The maximum magneto-optical signals caused by transitions of the main electrons in Ta (Figures 3 and 4) are reached at $h \approx 100$ nm. The exponential approximation of the far tail of the dependence $A(h)$ in Figure 3 allows estimating the length of spin diffusion of unexcited polarized electrons in tantalum as $\lambda_{sf} \approx 50 \pm 10$ nm. The extrapolation of the exponent at $h \to 0$ shows the magneto-optical signal generated only by the main electrons in permalloy, which is almost twice the amplitude of the resulting signal from both types of electrons. The value of λ_{sf} correlates with the dependence of the spin diffusion length $\lambda_{sf}(E-E_F)$ in Ta, calculated in Refs. [29,30] for excited electrons, with the extrapolation of the excitation energy $(E-E_F) \to 0$.

The diffusion of basic and non-basic polarized electrons from Py through the interface is accompanied by the diffusion of unpolarized electrons in the opposite direction to maintain electrical equilibrium. The rate of their polarization in Py is determined by the exchange energy and is much higher than the rate associated with diffusion, so the filling of the $d_{\uparrow\downarrow}$-subbands in Py does not change significantly and makes an insignificant contribution to the magnitude of the inverted signal.

Since the number of empty states in transition metals above the Fermi level E_F decreases as the d-shell of the element is filled [29], the magnitude of the inverted magneto-optical signal caused by transitions of non-basic electrons decreases from Ta to Pt. Consequently, the Kerr effect transformation decreases as the d-shell is filled in accordance with the experimental dependences of signals on thicknesses obtained in this paper for different normal metals and shown in Figure 5. As a result, platinum Pt(d^9), which is used in most studies of interfaces of $F|N$-structures, demonstrates the weakest Kerr signal inversion effect due to its high spin-orbit coupling and/or proximity to the para-ferromagnetic junction. The Cu layer (d^{10}) exhibits a shielding effect because d-band in copper is completely located below E_F.

Magneto-optical signals from Cu observed in Ref. [31] and from Au in Ref. [32] in two-photon experiments were most likely due to the release of electronic states in copper and gold, respectively, due to optical excitation of electrons and depletion of d-Cu and Au bands by the first optical pulse.

Compared with permalloy, iron has a 7-fold but opposite Kerr effect due to the wide empty d-band above the Fermi level for non-basic electrons, as shown in the box to Figure 6. In addition, the main charge carriers predominate in iron at the Fermi level. It can be expected that the Fe film will ensure the predominance of the main electrons in the non-magnetic metal in the $N|$Fe bilayer. On the other hand, in the case of the optical nature of the magneto-optical signal conversion, the dependence $A_{Ta}(h)$ for Ta|Fe should be identical to the dependence for Ta|Py, mirrored relative to the axis h, due to the similar optical parameters of iron

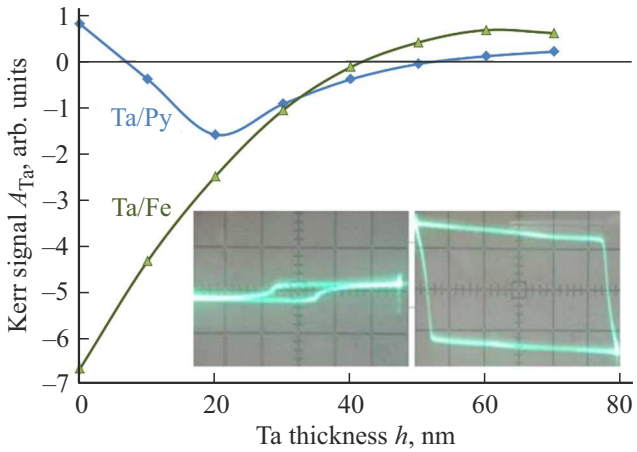

Figure 6. The dependences of the Kerr signals $A_{Ta}(h)$ on the thickness of the Ta h layer for the Ta|Py and Ta|Fe structures. The thickness of the Py and Fe layers is 30 nm. The insert shows the original Kerr signals from the individual layers Py (photo on the left) and Fe (photo on the right). Calibration of the magnetic field amplitude along the x axis — 4 Oe/div.

and nickel, but with a different Kerr signal sign. This makes it possible to use a comparison of the $A_{Ta}(h)$ dependencies for Ta|Fe and Ta|Py bilayers to elucidate the mechanism of the Kerr effect in a normal metal. Figure 6 shows both dependencies $A_{Ta}(h)$ for the Ta|Py and Ta|Fe bilayers.

It can be seen that the effect of converting the signal to Ta|Fe also occurs, including signal inversion. However, despite the close optical parameters of Py and Fe, there is no proportionality between the dependences for Ta|Py and Ta|Fe. The Kerr signal changes sign at a Ta thickness of $h \approx 40$ nm and reaches its maximum value at $h \approx 60$ nm, at which the light intensity in the Fe layer is vanishingly low.

The slow growth and positive sign of the inverted signal in the Ta|Fe bilayer at $h \geq 40$ nm allows drawing a natural conclusion about the proper contribution of the Ta layer to the Kerr signal due to diffusing main electrons from the Fe layer.

Evidence of Kerr signal formation in a non-magnetic metal is illustrated by hysteresis loops in Figure 7, which demonstrates the restoration of magneto-optical activity in a three-layer Ta|Al|Py structure by spraying a layer of tantalum on top of thick aluminum that does not transmit light. Al shields light in a similar way to Cu (Figure 5), while allowing polarized electrons to pass through almost losslessly [25].

In this experiment, the natural shielding effect of Al was observed- an exponential decrease in the signal with increasing aluminum thickness and its disappearance in the Al|Py structure when the thickness of Al exceeds the value ~ 40 nm. In this case, the majority of the Ta layer contains non-basic electrons, so that the signal in the three-layer Ta|Al|Py structure is inverted compared to the signal from permalloy and increases with increasing thickness of tantalum.

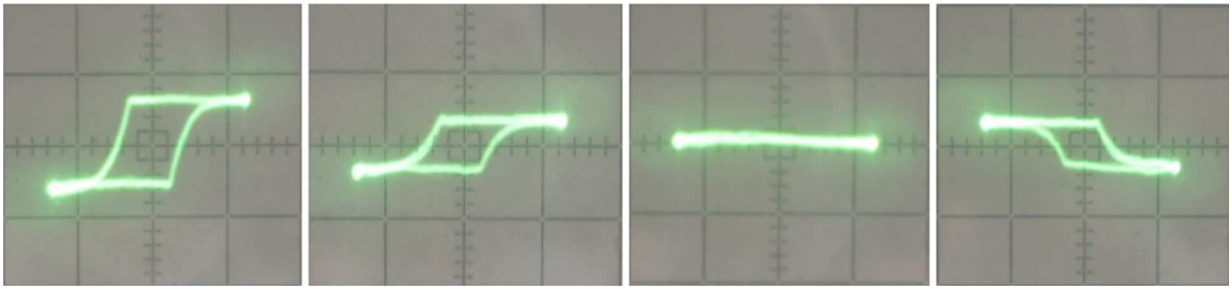

Figure 7. Restoration of a magneto-optical signal in a three-layer Ta|Al|Py structure, where the Al layer completely shields the signal from the Py layer: *a*) the initial signal from a single Py film with a thickness of 15 nm, *b*) signal from an Al|Py structure with a partially shielded Al layer 10 nm thick, *c*) zero signal from the Al|Py structure, completely shielded by an Al layer 40 nm thick, *d*) reconstructed inverted signal from the Ta|Al|Py structure after applying 20 nm thick Ta on top of a 40 nm thick Al shielding layer. Calibration of the magnetic field amplitude along the x axis — 4 Oe/div.

5. Conclusion

The possibility of observing the magneto-optical Kerr effect in films of non-magnetic transition metals up to ~ 200 nm thick deposited on the surface of a ferromagnetic metal at a light penetration depth not exceeding ~ 40 nm has been experimentally shown. Magneto-optical activity in non-magnetic metal films is related to the magnetization of the ferromagnetic layer. The magnitude of the Kerr signal in a non-magnetic metal depends on the elemental compositions of normal and ferromagnetic metals and may exceed the amplitude of the signal generated by the ferromagnetic film itself. The effect gradually weakens as the outer d- shell of ordinary metal ($d^2 \rightarrow \mathrm{d}^9$) is filled and disappears in metals with an empty or completely filled d-shell. The Kerr signal in the ferromagnetic metal layer is also modified by the ordinary metal underneath and can be amplified several times, especially for thin ($t \leq 10$ nm) magnetic films (Figure 4).

The most probable mechanism of transformation of the Kerr effect is the deep diffusion of unexcited polarized basic and non-basic electrons through the interface of two layers of ferromagnetic metal. At the same time, a normal transition metal does not show signs of ferromagnetism, which was established by neutronographic analysis. In a nonmagnetic metal, an equilibrium distribution of the concentration of polarized electrons diffusing from the ferromagnetic and relaxing in a normal metal is formed at the Fermi level with a zero gradient at the interface of the layers.

It should be noted that theoretical calculations of the parameters of carrier diffusion and relaxation in transition metals [30] concern only excited electrons, indicating that the spin diffusion length λ_{sf} is a function of the excitation energy. In this case, λ_{sf} $(E - E_F)$ tends to infinity if the excitation energy $(E - E_F)$ approaches zero.

The results of the study can be used to analyze the effects of spin accumulation near the interfaces of multilayer spin structures and their application in switchable elements, magneto-optical and plasmon sensors.

Acknowledgments

The author is grateful to E.S. Labutin for his help in preparing samples and to Yu.N. Khaidukov for PNR testing of bilayer structures, as well as to T. Rasing, V.A. Atsarkin, A.B. Granovsky, L.S. Uspenskaya and P.M. Vetoshko for fruitful discussions and comments.

Funding

This study was carried out under the state assignment of the National Research Center „Kurchatov Institute“.

References

[1] F. Hellman, A. Hoffmann, Y. Tserkovnyak, G.S.D. Beach, E.E. Fullerton, C. Leighton, A.H. MacDonald, D.C. Ralph, D.A. Arena, H.A. Dürr, P. Fischer, J. Grollier, J.P. Heremans, T. Jungwirth, A.V. Kimel, B. Koopmans, I.N. Krivorotov, S.J. May, A.K. Petford-Long, J.M. Rondinelli, N. Samarth, I.K. Schuller, A.N. Slavin, M.D. Stiles, O. Tchernyshyov, A. Thiaville, B.L. Zink. Rev. Mod. Phys. **89**, *2*, 025006 (2017).

[2] T.P.A. Hase, M.S. Brewer, U.B. Arnalds, M. Ahlberg, V. Kapaklis, M. Björck, L. Bouchenoire, P. Thompson, D. Haskel, Y. Choi, J. Lang, C. Sánchez-Hanke, B. Hjörvarsson. Phys. Rev. B **90**, *10*, 104403 (2014).

[3] T. Kuschel, C. Klewe, J.-M. Schmalhorst, F. Bertram, O. Kuschel, T. Schemme, J. Wollschläger, S. Francoual, J. Strempfer, A. Gupta, M. Meinert, G. Götz, D. Meier, G. Reiss. Phys. Rev. Lett. **115**, *9*, 097401 (2015).

[4] P. Bougiatioti, C. Klewe, D. Meier, O. Manos, O. Kuschel, J. Wollschläger, L. Bouchenoire, S.D. Brown, J.-M. Schmalhorst, G. Reiss, T. Kuschel. Phys. Rev. Lett. **119**, *22*, 227205 (2017).

[5] K.-S. Ryu, S.-H. Yang, L. Thomas, S.S.P. Parkin. Nature Commun. **23**, *5*, 3910 (2014).

[6] V.D. Zhaketov, D.I. Devyaterikov, M.M. Avdeev, D.A. Norov, E.D. Kolupaev, M.O. Kuzmenko, N.G. Pugach, Yu.N. Khaydukov, E.A. Kravtsov, Yu.V. Nikitenko, V.L. Aksenov. Phys. Solid State **65**, *7*, 1076 (2023).

[7] C. Stamm, C. Murer, M. Berritta, J. Feng, M. Gabureac, P.M. Oppeneer, P. Gambardella. Phys. Rev. Lett. **119**, 087203 (2017).

[8] D. Graulich, J. Krieft, A. Moskaltsova, J. Demir, T. Peters, T. Pohlmann, F. Bertram, J. Wollschläger, J.R.L. Mardegan, S. Francoual, T. Kuschel. Appl. Phys. Lett. **118**, *1*, 012407 (2021).
[9] O. Inyang, L. Bouchenoire, B. Nicholson, M. Toka c, R.M. Rowan-Robinson, C.J. Kinane, A.T. Hindmarch. Phys. Rev. B **100**, *17*, 174418 (2019).
[10] K.T. Yamada, M. Suzuki, A.-M. Pradipto, T. Koyama, S. Kim, K.-J. Kim, S. Ono, T. Taniguchi, H. Mizuno, F. Ando, K. Oda, H. Kakizakai, T. Moriyama, K. Nakamura, D. Chiba, T. Ono. Phys. Rev. Lett. **120**, *15*, 157203 (2018).
[11] W.L. Lim, N. Ebrahim-Zadeh, J.C. Owens, H.G.E. Hentschel, S. Urazhdin. Appl. Phys. Lett. **102**, *16*, 162404 (2013).
[12] S. Mironov, A.S. Mel'nikov, A. Buzdin. Appl. Phys. Lett. **113**, *2*, 022601 (2018).
[13] J. Xia, V. Shelukhin, M. Karpovski, A. Kapitulnik, A. Palevski. Phys. Rev. Lett. **102**, *8*, 087004 (2009).
[14] S. Hikino, S. Yunoki. Phys. Rev. Lett. **110**, *23*, 237003 (2013).
[15] F.S. Bergeret, A.F. Volkov, K.B. Efetov. Phys. Rev. Lett. **86**, *18*, 4096 (2001).
[16] T.S. Seifert, D. Go, H. Hayashi, R. Rouzegar, F. Freimuth, K. Ando, Y. Mokrousov, T. Kampfrath. Nature Nanotechnol. **18**, *10*, 1132 (2023).
[17] G. Armelles, A. Cebollada, A. Garcia-Martin, M.U. González. Adv. Opt. Mater. **1**, *1*, 10 (2013).
[18] T. Komesu, G.D. Waddill, J.G. Tobin. J. Phys.: Condens. Matter **18**, *39*, 8829 (2006).
[19] V.I. Safarov, V.A. Kosobukin, C. Hermann, G. Lampel, J. Peretti, C. Marliére. Phys. Rev. Lett. **73**, *26*, 3584 (1994).
[20] C. Hermann, V.A. Kosobukin, G. Lampel, J. Peretti, V.I. Safarov, P. Bertrand. Phys. Rev. B **64**, *23*, 235422 (2001).
[21] T.H.J. Loughran, P.S. Keatley, E. Hendry, W.L. Barnes, R.J. Hicken. Opt. Express **26**, *4*, 4738 (2018).
[22] L. Sapienza, D. Zerulla. Phys. Rev. B **79**, *3*, 033407 (2009).
[23] V.Ya. Gamlitskii, O.A. Gurkovskii, V.I. Nikolaev, I.N. Nikolaev, V.M. Cherepanov, S.S. Yakimov. JETP **40**, *2*, 374 (1975).
[24] E.K. Zavoiskii. JETP Lett. **21**, *7*, 191 (1975).
[25] A.G. Aronov. JETP Lett. **24**, *1*, 32 (1976).
[26] T. Katayama, Y. Suzuki, H. Awano, Y. Nishihara, N. Koshizuka. Phys. Rev. Lett. **60**, *14*, 1426 (1988).
[27] J.L. Erskine, E.A. Stern. Phys. Rev. Lett. **30**, *26*, 1329 (1973).
[28] V.P. Zhukov, E.V. Chulkov, P.M. Echenique. Phys. Rev. B **73**, *12*, 125105 (2006).
[29] I.A. Nechaev, V.P. Zhukov. Phys. Solid State **49**, *10*, 1811 (2007).
[30] V.P. Zhukov, E.V. Chulkov. Phys. Solid State **51**, *11*, 2211 (2009).
[31] A. Anadón, H. Singh, E. Díaz E.V. Chulkov, Y. Le-Guen, J. Hohlfeld, R.B. Wilson, G. Malinowski, M. Hehn, J. Gorchon. Phys. Rev. B **112**, *10*, 104437 (Phys. Solid State 2025).
[32] V.H. Ortiz, S. Coh, R.B. Wilson. Phys. Rev. B **106**, *1*, 014410 (2022).

Translated by A.Akhtyamov